Journal of the Nigerian Association of Mathematical Physics
Volume 63, (January – March, 2022 Issue), pp109 – 114

SOLAR ENERGY DRIVEN-PHOTOCATALYSIS: KINETICS AND SORPTION STUDIES OF Cr(VI) REDUCTION IN PAINT EFFLUENT

Osarumwense J. O and Chris-Abey O. F.

Department of Science Laboratory Technology, Faculty of Life Sciences, University of Benin, Benin City.

Abstract

Solar energy driven-photocatalysis is a clean and relatively new technology adopted to assuage the environmental problems caused by industrial effluent discharge. Chromium is widely used for the production of pigments for the paint and textile industries. The hexavalent form of chromium, Cr(VI) is highly toxic to human if ingested, and it is capable of causing oxidative damages to the blood cells at low concentration which may lead to hemolysis. In this study, a mixture of titanium oxide (TiO_2) and chromium contaminated effluent was irradiated under the sunlight for three hours in batch system. Some operational conditions such as catalyst dosage and exposure time were investigated during the photocatalytic process. Atomic absorption spectrophotometer (AAS) was used to determine the residual Cr(VI) ion in the mixture. The data obtained was subjected to a variety of kinetics models and adsorption equilibrium isotherms; the process was well modeled by pseudo-first kinetics order with a reaction rate constant of 0.0141 min^{-1}.The intra-particle diffusivity model revealed that the uptake of Cr(VI) ion was more of the film diffusion than the intra-particle diffusion. The data obtained from adsorption fitted well into the Langmuir adsorption isotherm with coefficient of determination (R^2) of 0.9387; while the Temkin isotherm indicates that the process was exothermic.

***Keywords*:** Solar energy, Photocatalysis, Chromium (VI), Adsorption equilibrium, Intra-particle diffusion.

1.0 Introduction

The photocatalysis facilitated by solar energy irradiated semiconductor oxide has been reported as a promising and useful technique for the removal of organic and inorganic contaminants in effluent [1]. Certain semiconductors are used for photocatalysis, and these include but not limited to TiO_2, ZnO, MgO, Fe_2O_3, and SnO_2. Semiconductors are materials with conduction and valence bands clearly separated by band-gap/ energy gap. When the energy absorbed is greater than or equal to band-gap of semiconductor, the electron in the valence band are excited, then moved up to conduction band. A charged carrier is generated. The properties for the semiconductor allow the substance to be used for photocatalytic studies [2].

Modified or unmodified TiO_2 stands out among the semiconductors used for the oxidation or reduction of gaseous and aqueous pollutants. This may results from the distinct properties exhibited by TiO_2, such as high photoactivity, photostability, chemically and biologically inert, not toxic, very good rate of adsorption/desorption and inexpensive [3]. However, it should be noted that UV/TiO_2 without the addition of an oxidant such as hydrogen peroxide in aqueous solution, produces a low quantum yield of hydroxyl radicals. TiO_2 catalyst activities can be improved by synthesizing TiO_2 with metal oxide such SnO_2, SiO_2, V_2O_3 to give nanoparticle such as TiO_2/Sn_2 [4]. The molecule of semiconductor absorbs photons (natural or artificial UV), and natural UV is obtained from sunlight. In tropical Countries, the highest level of global solar ultraviolet (UV) radiation is received for almost ten months of the year. Ultraviolet radiation wavelength ranges from 100 to 400 nm. The ultraviolet spectrum has been subdivided into different regions viz: UV-A (315 – 400 nm). This is the long wave ultraviolet and the major type of UV in sunlight. It is known as "blacklight". UV-B has wavelength range of 280-315nm. This is the dangerous part of sunlight. UV-C with wavelength range of 200 - 280nm, also known as shortwave UV; this is also a dangerous UV rays which includes a special UV-C (germicidal) at 253.7 nm wavelength known to kill airborne germs. The other type of UV is the UV-V also known as "vacuum UV" with wavelength below 200 nm [5].

The percentage of global UV radiation (direct and diffuse) increases generally with decreasing atmospheric transmittivity; this is mainly due to clouds, dust and aerosols. Most solar photocatalytic processes make use of the UV radiation of wavelength ranging from 300 to 400 nm. However, some photochemical synthesis can absorb solar rays up to 500 nm; though it was noted that the quantum yield of

Corresponding Author**:** Osarumwense J.O., Email: judeosarumwense@uniben.edu, Tel: +2348023297060

sunlight decreases as the wavelength increases [6]. The Photo-Fenton heterogeneous photocatalysis (a chemical combination of ferrous ions and hydrogen peroxide) and a propriety compound containing potassium ferrioxalate can absorb sunlight of wavelength up to 580 nm. Solar light of higher wavelength than 600 nm is not valid for photochemical process [7].

On the absorption of photoenergy (hv) greater or equal the band gap energy of semiconductor (3.2eV for anatase), electron (e^-) is excited from the valence band (VB) of the semiconductor to the conduction band (CB). Simultaneously, a negatively charged electron (e^-) vacancy or a positively charged hole (h^+) is created in the VB. The semiconductor then exhibits a region of void energy in which no energy levels are available for the promotion of the recombination of e^- and h^+ produced by photo-activation in the semiconductor [8]. A UV or near UV photons ($\lambda < 387$ nm) are required typically for this type of reaction [9]. The valence band h^+ is a strongly oxidizing agent, and the conduction band e^- is a strongly reducing agent. The excited e^- and h^+ can partake in reduction-oxidation processes with adsorbed species like water at the external surface. In general, h^+ oxidizes H_2O to ·OH (hydroxyl radicals), which initiates a series of reaction that leads to pollutant oxidation. Similarly, e^- is supplied to an acceptor like oxygen molecule, resulting in the formation of superoxide radical($O_2^{\cdot-}$). In photocatalytic processes, the ·OH was supposed to be the primary oxidant [10].

Chromium (VI) is hazardous to human and other organisms in the environment [11]. Because of its toxic nature, it is necessary to reduce its concentration in industrial effluent to acceptable level before discharge. Therefore, this study was focused on the photocatalytic removal of Cr(VI) in paint effluent using TiO_2 as catalyst under the sun.

Basically, Cr(VI) reduction by electron in solution (aqueous) will follow the reaction as stated in equation (1).

$$Cr^{6+} \rightarrow 3e^- + Cr^{3+} \quad (1)$$

It has been claimed that photocatalytic reduction of Cr(VI) can be achieved by directly capturing photo-generated electrons. However, it is realized by getting the electrons (Ti^{3+}) indirectly from the surface of TiO_2 catalyst [12]. If the species are first adsorbed on the surface of the photocatalyst, the electron transfer mechanism is more efficient [8, 13]. The reaction mechanism of the reduction of Cr(VI) photocatalytically is shown in equation (2) to (5) [14]

$$Cr^{6+}_{suspension} \rightarrow Cr^{6+}_{adsorbed} \quad (2)$$

$$TiO_2 + hv \rightarrow e^- + h^+ \quad (3)$$

$$Ti^{4+} + e^- \rightarrow Ti^{3+} \quad (4)$$

$$Ti^{3+} + Cr^{6+} \rightarrow Cr^{3+} + Ti^{4+} \quad (5)$$

1.1 Kinetics Model Equations

The experimental data will be subjected to some kinetics model equations such as intra-particle diffusion, pseudo-first order, and pseudo-second order equations in order to determine the kinetics parameters.

1.2 Pseudo first-order kinetics equation

$$\frac{d_q}{d_t} = K_1 (q_e - q_t) \quad (6)$$

q_t, q_e and k_1 are the amounts of Cr(VI) removed at time *t*, equilibrium per unit mass of the catalyst (mgg^{-1}) and pseudo first order kinetics rate constant respectively. After equation (6) has been integrated with boundary conditions ($t = 0\ to\ t = t\ and\ q_t = 0\ to\ q_t = q_t$) applied, it becomes:

$$log(q_e - q_t) = \log q_e - \frac{K_1}{2.303} t \quad (7)$$

Plotting $log(q_e - q_t)$ against *t* shows a linear relationship. k_1 is determined from the slope, and q_e from the intercept of the chart [15]

1.3 Pseudo second order kinetics equation

The kinetics equation of pseudo second-order is given as:

$$\frac{d_q}{d_t} = K_2 (q_e - q_t)^2 \quad (8)$$

The rate constant is K_2 ($gmg^{-1}min^{-1}$). Linearizing the above equation gives

$$\frac{1}{q_e - q_t} = \frac{1}{q_e} + K_2 t \quad (9)$$

Further rearrangement of equation (9) gives the following:

$$\frac{t}{q_t} = \frac{1}{K_2 q_e{}^2} + \frac{1}{q_e} t \quad (10)$$

but

$$h = k_2 q^2 \quad (11)$$

where h is the initial sorption rate (mgg^{-1}). Plotting t/q_t against *t* yields a straight line, and k_2 is determined from the chart [16].

1.4 Intra particle diffusion

The equation of intra-particle diffusion was used to investigate the mechanism of diffusion during photocatalytic process [17]. The following equation was proposed by Crank [18].

$$q_t = K_{id}\, t^{0.5} \quad (12)$$

The coefficient k_{id} is obtained from the plot of q_t versus $t^{0.5}$ [19]. The plot of equation (12) is supposed to be linear passing through the origin; however, if the plot is not linear and does not pass through the origin, then the intra-particle diffusion cannot be assumed as the only mechanism involved in the diffusivity [20]. According to report obtained from previous research [21], if the intra-article diffusion plot does not pass through the origin, equation (12) becomes:

$$q_t = K_{id}\, t^{0.5} + C_{id} \quad (13)$$

where C_{id} is the intercept of the chart, and it is known as the intra-particle diffusion constant. Apart from the linearity of the plot, mechanism of sorption assumes intra-particle diffusion for the following conditions: high coefficient of determination (R^2), indicating applicability, straight line passing through the origin and intercept $C_{id} < 0$. Deviation from the above conditions gives an indication that the transport mode is affected by more than one process.

1.5 Adsorption Isotherms

For single metal adsorption, some isotherm equations were used to establish the adsorption isotherms of photocatalytic reduction of Cr(VI).

1.6 Freundlich Isotherm

The experimental data often fit to the empirical Freundlich Isotherm as shown in equation (14) and (15). This is commonly used to describe the characteristics of adsorption for the heterogeneous surface. The associated constants in the Freundlich isotherm are the sorption intensity $(1/n)$ and sorption capacity (K_f). These parameters provide an indication for the favorability of the isotherm. C_e is concentration of the photocatalyst at equilibrium (mgL^{-1}), q_e is amount of metal adsorbed per one gram of the catalyst at equilibrium (mgg^{-1}) [22].

$$q_e = K_f\, C_e^{1/n} \qquad (14)$$

$$log\ q_e = log\ K_f + \frac{1}{n}\log C_e \qquad (15)$$

The value of $(1/n)$ ranges from 0 and 1. It measures surface heterogeneity. The system becomes more heterogeneous as the value move closer towards zero [23]. If $(1/n)$ is equal to 1, it means that the concentration is independent of partition between the two phases. If (^{1}/n) is below 1, it means a normal adsorption but a cooperative adsorption, if the value is above one [24].

1.7 Langmuir Isotherm

The Langmuir proposed the following transformed and linearized equation:

$$\frac{1}{q_e} = \frac{1}{Q_o} + \frac{1}{Q_o\, K_L C_e} \qquad (16)$$

C_e is the concentration of adsorbate (mgL^{-1}) at equilibrium, q_e is the metal adsorbed by the semiconductor per gram at equilibrium (mgg^{-1}) and Q_o is the monolayer capacity (mgg^{-1}). K_L is Langmuir isotherm constant (Lmg^{-1}). K_L and Q_o are obtained from the intercept and slope of the Langmuir plot [25]. R_L is an essential features of the Langmuir isotherm, It is a dimensionless constant known as separation factor.

$$R_L = \frac{1}{1 + (K_L C_o)} \qquad (17)$$

The R_L value indicates the shape of the isotherm. When R_L is 1, isotherm is termed to be linear; $R_L > 1$, isotherm is unfavorable; it is irreversible when R_L is 0 and favorable when $0 < R_L < 1$. [26].

1.8 Temkin Isotherm Model

The Temkin isotherm model looks into the effect of indirect adsorbent/ adsorbate interaction on the photocatalytic process; and it is assumed that heat of adsorption (ΔH_{ads}) of molecules in the layer decreased linearly as the coverage area increases [26]. Temkin model tests the adsorption potential of TiO_2. The linear form of Temkin isotherm is given in equation (18):

$$q_e = \frac{RT}{b_T}\, In\, K_T + \frac{RT}{b_T}\, In\, C_e \qquad (18)$$

Where, R is gas constant, t is the absolute temperature (K), the Temkin constant is $1/b_T$ which is related to the heat of sorption (KJ/mol.), while K_T (L/g) is related to adsorption capacity.

2. Materials and methods

2.1 Materials

TiO_2 and other reagents used in this investigation were of analytical grades obtained from pyrex scientific limited, Benin City. Wastewater was collected from paint manufacturing industry in Benin City. The photocatalytic studies were carried out following the method adopted from previous work [27]. The experiment was carried out under the sun within three hours (12 noon to 3 pm) using a flat surface orbital shaker (Model OS-752, Optima, Japan). Prior to the photocatalytic studies, Atomic absorption spectrophotometer (AAS) (solar 140 models, manufactured by Laboratory exchange Company Limited, United Kingdom) was used to determine the initial concentration of chromium ion in the paint effluent.

2.2 Photocatalytic Reduction Studies

The photocatalytic studies were carried out under sunlight on the orbital shaker operated at a speed of 120 rpm for continuous agitation. The effect of catalyst (TiO_2) dosage on the photocatalytic reaction was carried out by mixing 200 mL of paint effluent with varying amount of TiO_2 (0.25 – 1.25 gL^{-1}) in five different 500 mL Erlenmeyer flasks. A sixth flask (control) containing 200 mL of the effluent but no catalyst was added. The flasks were agitated for three hours. Samples were collected from each flask at predetermined time to assess the impact of irradiation time and catalyst dosage, the samples were filtered using fine crystalline filter paper, and the residual concentration of chromium ion was determined using Atomic absorption spectrophotometer [27]. The experiment was repeated in the laboratory without the use of sunlight, with the conical flasks coated in aluminum foil to prevent UV radiation penetration [28].

3. Results and Discussion

In order to investigate the effects of sunlight and catalyst on Cr(VI) reduction, control experiments were carried out. One set of experiment was carried out under the sun (UV only), another set was done with TiO_2 (1.0 mg/L) in the laboratory without sunlight (catalyst only) and the third set was performed in the presence of sunlight and catalyst (UV/TiO_2) as shown in Figure 1. From the result, there was indication that sunlight and catalyst played prominent roles in the photocatalytic reduction process of Cr(VI). About 78% reduction of Cr(VI) was obtained with UV/TiO_2 as against 49% with TiO_2, while no significant reduction was observed with UV only. This is in agreement with the report of the previous studied which stated that photocatalysis is initiated by photon energy (UV rays) with a stable metal oxide as catalyst [1].

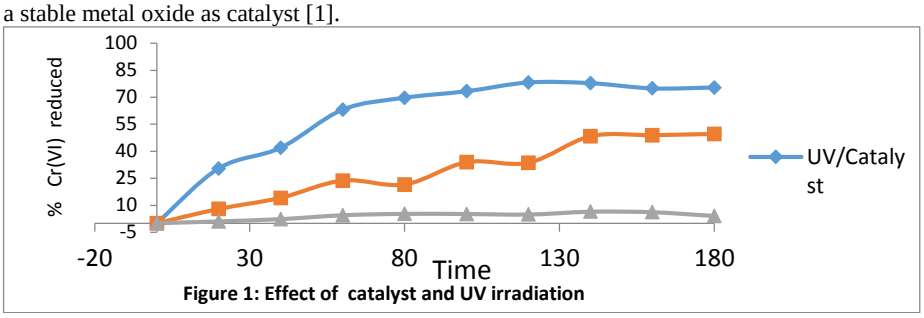

Figure 1: Effect of catalyst and UV irradiation

The effect of irradiation time and catalyst dosage on the photocatalytic reduction of Cr(VI) were investigated. Figure 2 shows the concentration profile of Cr(VI) at various dosage. From the chart, it was observed that the reduction of Cr(VI) was rapid within the first 60 minutes; it became slower and almost constant at 140 minutes. At this point, the process was almost at equilibrium. At 140 minutes of exposure to sunlight, the Cr(VI) was reduced from initial concentration of 1.18 $mgdm^{-3}$ to 0.64 $mgdm^{-3}$ at catalyst dosage of 0.25%. The same trend was observed with the other catalyst dosages. Greater photon was absorbed by the catalyst at elongated irradiation time corresponding to higher reduction of Cr(VI) in the effluent.

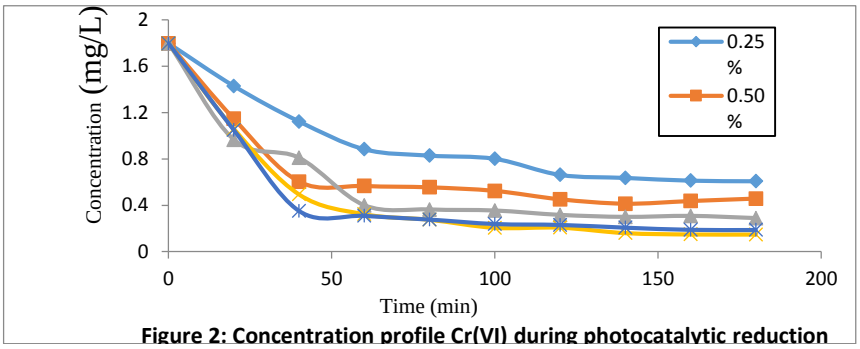

Figure 2: Concentration profile Cr(VI) during photocatalytic reduction

Similarly, increased catalyst dosage may have increased the number of active sites on the catalyst surface, resulting to the increase in quantity of free radicals (OH) in solution. This in turn increased the photo-redox reaction of the substrate in the effluent sample [29].

3.1 Kinetics and Adsorption Isotherms Models

To establish the equilibrium parameters and kinetics, as well as the rate-limiting stage of the photocatalytic process, kinetics and adsorption studies were carried out. The experimental data were subjected to various kinetics and adsorption models. Table 1 shows the rate constants and other parameters obtained from the linear plots of the kinetics equations. The kinetic rate constants and coefficient of determination (R^2) values suggested that the pseudo first-order model fit the process better than the pseudo second-order model. The pseudo first-order kinetics model had a rate constant (k_1) of 0.0194 min^{-1} and an R^2 of 0.9539 at a catalytic dose of 1 gL^{-1}, while the pseudo second-order kinetics model had a rate constant (k_2) of 1.4 10^{-2} $gmg^{-1}min^{-1}$ and an R^2 of 0.8157. The same trend was observed in previous work [30].

The intra-particle diffusion often plays an important role in adsorption especially for porous adsorbent. It is a transport process which involves the movement of species from the bulk of the solution to the solid phase [31]. In Figure 3, the linear plot of intra-particle diffusion equation, gives the rate constant of 0.1810 $gmg^{-1}min^{0.5}$. The regression lines did not pass through the origin, therefore an intercept C_{id} was provided. This is an indication that the reaction was a rate-limiting steps other than intra-particle diffusion. In addition, the K_{id} value was greater than zero, indicating that both external mass transfer (film diffusion) and intra-particle diffusion were considered as rate limiting steps [21].

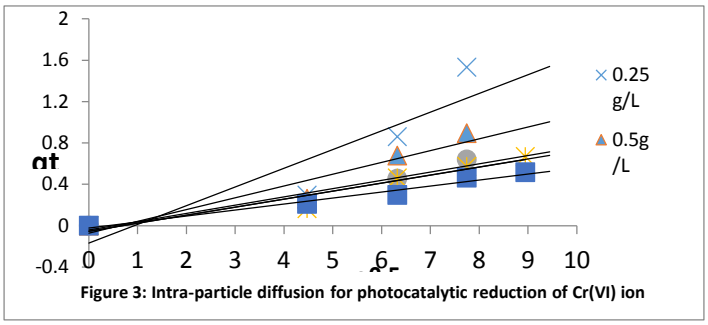

Figure 3: Intra-particle diffusion for photocatalytic reduction of Cr(VI) ion

Table 1: The photocatalytic kinetics for the reduction of Cr(VI) in industrial effluent

	Pseudo first-order		Pseudo second-order		Intra-particle diffusion		
Catalyst dosage	K_1 (min^{-1})	R^2	K_2 ($gmg^{-1}min^{-1}$)	R^2	K_{int} ($gmg^{-1}min^{0.5}$)	C_{id} (mgg^{-1})	R^2
0.25 gL^{-1}	0.0134	0.9383	2.90E-2	0.9118	0.1723	-0.1763	0.8785
0.50 gL^{-1}	0.0158	0.9687	3.02E-2	0.8914	0.1436	-0.0674	0.9192
0.75 gL^{-1}	0.0127	0.9677	4.36E-2	0.9081	0.0989	-0.04430	0.9437
1.00 gL^{-1}	0.0141	0.9350	2.24E-2	0.9007	0.09747	-0.0556	0.9183
1.25 gL^{-1}	0.0153	0.9578	2.52E-2	0.9079	0.0884	-0.02332	0.9084

Prior to UV illumination, the contaminant was pre-adsorbed on the surface of the catalyst for the adsorption isotherm and photocatalysis mechanism [2]. Table 2 shows the isotherm parameters and correlation coefficients. The best description for Cr(VI) adsorption on TiO_2 was the Langmuir isotherm, which had a regression value (R_2) of 0.9387, and sorption capacity of 1.56 Lmg^{-1}. In this investigation, the R_L value (0.1584) was between 0 and 1, indicating that the adsorption was favorable [26]. The Freundlich model's adsorption strength ($^1/n$) also implied that the adsorption process was favorable [32]. The Temkin model parameters K_T and b_T were obtained; b_T, also known as the heat of sorption, yielded a positive value of 3.012 $KJmol^{-1}$, suggesting that the process of adsorption was exothermic. This aligned with the findings of previous work carried out by other researcher [33].

Table 2: Adsorption isotherm parameters for photocatalytic reduction of Cr(VI) in paint effluent

Langmuir	Value
K_L	1.73
R^2	0.9387
R_L	0.1584
Freundlich	
K_f (mgg^{-1})	1.43
R^2	0.9381
$^1/n$	0.7853
Temkin	
K_T (Lmg^{-1})	10.84
B_T $(kJmol^{-1})$	3.012
R^2	0.9143

4. Conclusion

Solar irradiation was proven to be effective for the photoreduction of Cr(VI) ion in paint manufacturing effluent employing TiO_2 catalyst in this study. Within three hours of continuous agitation, 78 % of the Cr(VI) ion was reduced using UV/TiO_2 as against 49% with TiO_2 only. Pseudo-first order kinetics models accurately described the photocatalytic reduction of Cr(IV) using TiO_2. The uptake of Cr(VI) ion was more of a film diffusion than an intra-particle diffusion, and the adsorption fitted well into the Langmuir adsorption isotherm, whereas the Temkin isotherm indicated that the process was exothermic.

5. Acknowledgement

We wish to express our gratitude to the staff of Department of Chemistry, Faculty of Physical Sciences, University of Benin, Benin City where the AAS analysis was carried out. We also wish to acknowledge the staff of Science Laboratory Science, Faculty of Life Sciences, University of Benin, Benin City for providing the laboratory for this study.

6. References

[1] Amenaghawon, N. A., Osarumwense, J. O., Aisien, F. A. and Olaniyan, O. K. (2014). Preparation and investigation of the photocatalytic properties of periwinkle shell ash for tartrazine decolourisation. *Journal of Mechanical Engineering and Sciences*, 7: 1070-1084.

[2] Lin, H. and Valsaraj, K. T. (2005). Development of an optical fiber monolith reactor for photocatalytic wastewater treatment. *Journal of Applied Electrochemistry*, **35** (7): 699-708.

[3] Inamdar, J. and Singh, S. K. (2008). Photocatalytic detoxification method for zero effluent discharge in dairy industry: Effect of operational parameters. *International Journal of Chemical and Biological Engineering*, **1**(4): 160-164.

[4] Khuanmar, K., Wirojanagud, W. Kajitivichyaukul, P. and Maensiri, S. (2007), Photocatalysis of Phenolic Compounds with synthesized Nanoparticle TiO_2/Sn_2. *Journal of Applied Sciences*, (14): 1968-1972.

[5] Barbero, F. J., Lopez, G. and Batlles, F. J., (2006), Determination of Daily Solar Ultraviolet Radiation using Statistical Models and Artificial Neural Networks, *Annals of Geophyics*, 24:21205-2114.

[6] Mehos M. and Turchi C. (1992). Measurement and analysis of near ultraviolet solar radiation. Solar Energy. 1: 51-55.

[7] Malato, S. (2004), Photocatalytic reactors for the treatment of liquid wastewater in the presence of solar irradiation, *Thessalonica.* 1-15.

[8] Linsebigler, A. L., Lu, G. and Yates, J. T. (1995). Photocatalysis on TiO_2 Surfaces: principles, mechanisms, and selected results. *Chemical Reviews*, 95: 735-758.

[9] Priya, S. S., Premalatha, M. and Anantharaman, N. (2008). Solar Photocatalytic Treatment of phenolic wastewater potential, Challenges and Opportunities. *Journal of Engineering and Applied Sciences*, 3(6): 36-41.

[10] Kavita K., Rubina, C. and Rameshwar, L. S. (2004). Treatment of hazardous organic and inorganic compounds through aqueous-phase photocatalysis: A Revie. *Industrial and Engineering Chemistry Research*, 43: 7683-7696.

[11] Shaban, Y. A. (2013). Effective photocatalytic reduction of Cr (VI) by carbon modified (CM)-n-TiO_2 nanoparticles under solar irradiation. *World Journal of Nano Science and Engineering*, 3: 154-160.

[12] Liu, S. X., Qu, Z. P., Han, X. W. and Sun, C. L. (2004). A mechanism for enhanced photocatalytic activity of silver-loaded titanium dioxide," *Catalysis Today*, 93(5): 877–884.

[13] Idris, A., Hassan, N. Rashid, R. and Ngomsik, A. F. (2011). "Kinetic and regeneration studies of photocatalytic magnetic separable beads for chromium (VI) reduction under sunlight," *Journal of Hazardous Materials*, 186(1): 629–635.

[14] Ma, C. M., Shen, Y. S. and Lin, P. H. (2012). Photoreduction of Cr(VI) ions in Aqueous Solutions by UV/TiO_2 Photocatalytic Processes. *International Journal of Photoenergy*, 1-7

[15] Martins, R. J. E., Vilar, V. J. P. and Boaventura, R. A. R. (2014). Kinetics modelling of cadmium and lead removal by aquatic Mosses. *Brazilian Journal of Chemical Engineering*, **31**(1): 229-242.

[16] Adeyi, O., Sunday, O., Ayanda, G. O. and Ganiyu, O. (2013). Adsorption kinetics and intra particulate diffusivity of aniline blue dye onto activated plantain peels carbon. *Chemical Science Transactions*, 2(1): 294-300.

[17] Gerente, C., Lee V. K. C., Le Cloirec, P. and McKay, G. (2007). Application of chitosan for the removal of metals from wastewaters by adsorption – mechanisms and models review. *Critical Reviews in Environmental Science & Technology*, 37: 41–127.

[18] Crank, J. (1970). *Mathematics of Diffusion*. Clarendon Press, Oxford, p.416.

[19] Ho, Y. S. and McKay, G. (1999). The sorption of Lead (II) ions on Peat. *Water Research*, **33(**2): 578–584.

[20] Perju, M. M. and Dragan, E. S. (2010). Removal of azo dyes from aqueous solution using chitosan based composite hydrogels. *Ion Exchange Letters*, 3: 7 – 11.

[21] Itodo, A. U., Abdulrahman, F. W., Hassan, L. G., Maigandi, S. A. and Itodo, H. U. (2010). Intra-particle diffusion and intra-particulate diffusivities of herbicide on derived activated carbon. *Researcher*, 2(2):74-86.

[22] Hutson, N. D. and Yang, R. T. (2000). Adsorption. *Journal of Colloid Interface Science*, 189-195.

[23] Foo, K. Y. and Hameed, B. H. (2010). Insight into the models of adsorption isotherm systems. *Chemical Engineering Journal*, 156:2-10.

[24] Voudrias, E., Fytianos, F. and Bozani, E. (2002). Sorption description isotherms of dyes from aqueous solutions and Wastewater with different sorbent materials, *Global Nest, The International Journal*, 4(1): 75-83.

[25] Dada, A. O., Olalekan, A. P., Olatunya, A. M. and Dada, O. (2012). Langmuir, Freundlich, Temkin and Dubinin Radushkevich isotherms studies of equilibrium sorption of Zn^{2+} unto phosphoric acid modified rice husk. *Journal of Applied Chemistry*, 3(1): 38-45.

[26] Elmorsi, T. M. (2011). Equilibrium isotherms and kinetic studies of removal of methylene blue dye by adsorption onto *Miswak* leaves as a natural adsorbent. *Journal of Environmental protection*, 2:817-827.

[27] Osarumwense, J. O. and Ejoboka O. L. (2016). Kinetics and sorption modelling of photocatalytic removal of Pb(II) in paint effluent using TiO_2 under solar irradiation. *Journal of the Nigerian Association of Mathematical Physics*, 33: 167-178.

[28] Crittenden, J. C., Zhang, Y., Hand, D. W., Perram, D. L. and Marchand, E. G. (1996). Solar detoxification of fuel-contaminated groundwater using fixed bed photocatalysts. *Water Environment Research*, 68: 3, 270-278.

[29] Rahimi, S., Ahmadian, M., Barati, R., Yousefi, N., Moussavi, S. P., Rahimi, K., Reshadat, S., Ghaseni, S., Gilani, N. R. and Fatehizadeh, A, (2014). Photocatalytic removal of cadmium (II) and lead (II) from simulated wastewater at continuous and batch system. *International Journal of Environmental Health Engineering*, 3(2): 90-94.

[30] Daneshvar, N., Aber, S., Seyed Dorraji, N. S., Khataee, A. R. and Rasoulifard, M. H. (2007). Preparation and Investigation of Photocatalytic Properties of ZnO Nanocrystals: Effect of Operational Parameters and Kinetic Study, *World Academy of Science, Engineering and Technology*, **29**:267-272.

[31] Randhawa, N. S., Das, N. N and Jana, R. K. (2013). Adsorptive remediation of Cu(II) and Cd(II) contaminated water using manganese nodule leaching residue, *Desalination and water treatment*, 22-24(52):4197-4211.

[32] Mohan, S. and Karthikeyan, J. (1997). Removal of lignin and tannin color from aqueous solution by adsorption on to activated carbon solution. *Environmental Pollution*, 97**:** 183-187.

[33] Negrulescu, A., Patrulea, V., Mincea M. and Moraru, C. (2014). The adsorption of tartrazine, congo red and methyl orange on chitosan beads. *Digest Journal of Nanomaterials and Biostructures*, 9:45-52.